Dalton Transactions

Accepted Manuscript

ROYAL SOCIETY OF CHEMISTRY

www.rsc.org/dalton

Journal Name

RSCPublishing

COMMUNICATION

Facile preparation and bifunction imaging of Eu-doped $GdPO_4$ nanorods with MRI and cellular luminescence

Cite this: DOI: 10.1039/x0xx00000x

Qijun Du[a], Zhongbing Huang[a]*, Zhi Wu[a], Xianwei Meng[b]*, Guangfu Yin[a], Fabao Gao[c], Lei Wang[c]

Received 00th January 2014,
Accepted 00th January 2014

DOI: 10.1039/x0xx00000x

www.rsc.org/

The biocompatibility of nanomaterials with multi-functions is very important for their clinical applications. Herein, the hexagonal crystal Eu−doped $GdPO_4$ nanorods (NRs) in the template of silk fibroin (SF) peptides are successfully synthesized via a mineralization process. The sizes of the Eu-doped $GdPO_4$ NRs with SF peptides (SF-NRs) are the length of ~150 nm and the diameter of ~10 nm. The Eu-doped SF-NRs have strong pink luminescence and the mass magnetic susceptibility value (1.27 emu/g in 20000 G of magnetic field) due to Eu ions doping. The cell test indicates that the Eu-doped SF-NRs obviously promote the viability of cells at NRs concentration of 25-200 μg/mL. A growth mechanism of Eu-doped $GdPO_4$ SF-NRs is proposed, to explain their strong cellular luminescence, magnetic resonance (MR) imaging and good cyto-compatibility. Compared to NRs without SF, the Eu-doped SF-NRs not only exhibit a higher effective positive signal-enhancement ability (the longitudinal relaxivity r_1 value is 1.38 (Gd mM·s)$^{-1}$) and *in vivo* T_1 weighted MR imaging enhancement under a 7.0 T MRI system, but also show the better luminescence imaging of living cells under the fluorescence microscope, indicating that the Eu-doped SF-NRs have potential as T_1 MRI contrast agents and optical imaging probe.

Recently, luminescent nanomaterials of rare earth have been prepared and applied in many fields.[1] By controlling the reaction conditions, their different nanostructures could be obtained, such as hollow microspheres, nanorods (NRs), nanowires, and nanobelts of $LnPO_4$. Due to their unique properties, $LnPO_4$ can be applied in a various of fields, such as luminescence or laser nanomaterial, magnets, heat-resistant materials, biochemical probes and medical diagnostics.[2]

Multimodal bio-imaging is a new technique, which combines with more than one imaging modality together, such as optical imaging, magnetic resonance imaging (MRI), positron emission tomography, X-ray computed tomography, and ultrasound.[2] Because of the use of organic dyes, quantum dots or Ln^{3+} doping, optical imaging can provide sensitivity and spatial resolution, but it lacks the full capability of acquiring depth and anatomic details.[3] Lanthanides-based nanomaterials can be used as MRI contrast agents to provide bright MRI signal.[4] Although MRI is restrained by sensitivity and spatial resolution of an imaging technique at the cellular level,[5] luminescent image from MRI contract agents can improve cell resolution. $LnPO_4$ exhibits electronic and optical characteristics arising from 4f electrons, which are well shielded by $5s^2p^6$ shell, leading to their luminescence. $GdPO_4$-based nanoparticles (NPs) have the potential to be used in MRI,[1b,1i] and doping can offer these NPs a bridge gaps to combine of MRI and optical imaging. For example, dextran-coated $GdPO_4$ NRs are prepared to be used as T_1 MRI contrast agents,[6] and $GdPO_4$ hollow spheres could be used in optical imaging.[1h] Recently, europium (II) analogues have been proposed as alternatives to Gd ions due to their isoelectronic—each having seven unpaired electrons.[7] Although Eu^{3+} is a poor relaxation agent compared to Gd^{3+} and Eu^{2+}, Eu^{3+} is an efficient luminescent species, which can be applied in the Gd^{3+} analogues for a structural probe.[8] Because Eu^{3+}-doped phosphors exhibit broad excitation band and excellent thermal stability,[3] combining the paramagnetism of $GdPO_4$ with the fluorescence of the doping ions (Eu^{3+}) can tailor the multi-functions of the nanomaterial. However, many state-of-the-art surface functionalization methods afford high-quality bioprobes by post-modification on pre-synthesized nanomaterials, namely, by a multi-step route, which is always very tedious and complex [1a,1b,1h,1i,1k]. Silk fibroin (SF) with histidine and lysine can induce to fabricate metal compounds nanoparticles.[11] Up to now, success on facile and efficient one-step preparation of SF–coated $GdPO_4$ NRs is very challenging.

Surface modification can facilitate the biocompatibility to nanomaterials for reducing their toxicity and avoiding their metal-ion release in the body. Modification methods include the interaction between avidin/biotin and the specific groups on the NPs surface.[11,9] A mild room-temperature synthesis method mimicking the natural bio-mineralization process has been developed, in which bio-molecules are used as the structure-directing agent to control the nucleation and subsequent crystal growth, and eventually to yield unique biomolecule-composited micro- or nano-structure with high surface-to-volume ratio and good bio-compatibility.[10,11] For example, the DNAs, proteins, peptides, amino acid molecules etc. were used as templates to prepare NPs in normal pressure and temperature. In our previous works, ZnO NPs, Ni-doped ZnO NPs, GaOOH nanorods (NRs)

and $ZnFeO_4$ NPs with biocompatibility were prepared successfully at room temperature in the presence of SF peptides.[11] SF is one of the most extensively used biomaterials due to its good biocompatibility, and it can be hydrolyzed into the peptides, providing nucleophilic hydroxyl groups of amino acids, which are very important in the nucleation process of biomineralization.[11b] Talham et al.[12] et al prepared DNAs-modified $GdPO_4$ NRs as MRI contrast agents. Recently, Talham et al.[4b] further modified $Eu_{0.2}Gd_{0.8}PO_4{\cdot}H_2O$ NPs using phosphonomethyl iminodiacetic acid, and found their size-dependent MRI relaxivity and fluorescence image. However, success on facile and efficient one-step preparation of peptide-modified $GdPO_4$ NRs with bifunctions is not reported, and remains challenge. Herein we report a kind of dual-functional Eu-doped $GdPO_4$ NRs with SF (named as SF-NRs) prepared via a one-step mineralization process, and assess the potential of these NRs as the bimodal of luminescence/MRI. Since these Eu-doped $GdPO_4$ SF-NRs could be used as micro imaging tools at the cellular level, the interactions between SF-NRs and living cells of L929 need to be investigated.

In Figure 1a and b, it is found that the prepared Eu-doped $GdPO_4$ NRs with SF have 160 ± 20 in length and 15 ± 10 nm in diameter, while the size of NRs without SF is 150 ± 30 in length and 10 ± 12 nm in diameter. Length distributions of Eu-doped NRs with and without SF in Figure S1 could indicate that SF peptides can increase the length of the as-prepared Eu-doped NRs, and each distribution is determined from more than 200 objects based on a series of SEM images. In Figure 2c, the XRD patterns can be indexed as the hexagonal phase of $GdPO_4{\cdot}H_2O$ (JCPDS No.39-0232) and hexagonal $EuPO_4{\cdot}H_2O$ (JCPDS No.20-1044),[13] and the peaks in the pattern of SF-NRs are stronger than those of samples without SF. The crystallites sizes evaluated from Sheller equation for SF-NRs and NRs without SF are 10.6 nm and 9.7 nm, respectively; and the crystallization degree in SF-NRs and NRs without SF (calculated from software JDDE 6.5) are 74.23 % and 70.79 %, respectively. These results further indicate that SF peptides could promote the crystallization in the growth time of NRs. Raman spectra of as-synthesized hexagonal NRs with and without SF are shown in Figure 1d. The most intense Raman band of the rhabdophane-type NRs is 993 cm^{-1}, which is assigned to the A mode, with totally symmetric vibration.[2b,4b] The Raman bands at 472 cm^{-1} and 1103 cm^{-1} are the A_g and B_g mode, respectively. These peaks (at 472, 993 and 1103 cm^{-1}) of SF-NRs are stronger than those of NRs without SF, which should result from two facts, on one hand, "electromagnetic" field enhancement or "chemical first-layer" effects[11f,12] due to the coordination of Gd^{3+} and the carbonyl group of SF, on the other hand, the higher crystallization degree in SF-NRs due to the induction effect of SF peptides. Fourier transform infrared (FT-IR) spectra confirm successful conjugation with SF chains. The result of EDS spectrum in Figure S1b and (FT-IR) spectra (Figure S2) also shows the existence of SF peptides in the $Eu_{0.2}0Gd_{0.8}PO_4$ SF-NRs. In Figure S2, the band at 3540 cm^{-1} arises from the stretching modes of the OH groups, and the smaller peaks at 2930 and 2847 cm^{-1} are the asymmetric (ν_{as}) and symmetric (ν_s) stretching vibration of C-H_3 in SF chains, indicating that there are many hydroxyl groups and SF chains in/on the SF-NRs. The broad and high-intensity band extending from 2500 to 3600 cm^{-1} derives from the ν_3 and ν_1 stretching modes of the hydrogen-bonded H_2O molecules, and the band at 1620 cm^{-1} (from the ν_2 bending mode of H_2O molecule) of SF-NRs is stronger than that of the NRs without SF, indicating that there might be more water molecules absorbed on the surface of SF-NRs due to the existence of SF chains. Figure 1e and f show TG-DSC curves of the doped NRs in the temperature range of 30-800 °C. The mass decrease before around 200 °C indicates the dehydration of the prepared NRs, and the further mass decrease after 200 °C indicates the dehydroxylation in the prepared NRs. In the DSC curves, the endothermic peak (at around 175.4 °C) of SF NRs is stronger than that (at around 185.8 °C) of NRs without SF, indicating that there is a degradation process of SF on the NRs during the dehydration. In general, the result of NRs without SF shows about a 7.46 % loss in weight (Figure 1f); however, the weight loss reached a value of 8.50% in NRs with SF (Figure 1e), indicating that about 1 % is a loss result of SF peptide during the calcination. These results further indicate that there were SF peptides in SF-NRs.

The composition of the as-prepared NRs is analyzed by the XPS, and Figure 2a, b and Table S1 show the element contents of the doped NRs with/without SF. The results indicate the existence of Gd, Eu, P and O in the rods, suggesting that there are 0.86 atom% of Eu ions existed on/in SF-NRs, and 0.241 ratio of Eu/Gd in SF-NRs is more than 0.218 ratio of Eu/Gd in NRs without SF. Furthermore, the element C in the as-prepared sample mainly results from the SF coated on the NR surfaces, and 8.77% of N atoms mainly result from the NO_3^- groups in $Gd(NO_3)_3$. However, the 1.27% of C atoms in NRs without SF result from the impure C in the measuring environment, and the excessive O atoms result from OH^- groups and the absorbed water on the NRs surfaces. These results indicate that SF may also induce more Eu ions to enter into/onto the $GdPO_4$ NRs. To further investigate the chemical environment of two samples, high-resolution spectroscopy on Eu (3d) was performed. In Figure S3, the stronger peak at 1137 eV and the weaker peak at 1127 eV are attributed to Eu^{3+} $3d_{5/2}$ and Eu^{2+} $3d_{5/2}$, respectively, and the peak area of Eu^{2+} in the pattern of SF-NRs (Figure S3a) is larger than that of NRs without SF (Figure S3b), suggesting that there are more Eu^{2+} ions existed on the SF-NRs surface. The appearance of Eu^{2+} might result from the redox of Cl^- ions (from $EuCl_3$)[14] and tyrosine[15] in SF peptides. In the HRTEM images of Figure 2c–f, the lattice spaces of Eu-doped $GdPO_4$ NRs are calculated to be 0.63 nm, which coincide well with distances of (001) lattice plane of hexagonal $GdPO_4$ crystal. Figure 2c and 2d show SF peptides (marked by the green arrows), and the diameter of SF-NR is about 6.5 nm. However, the diameter of NRs without SF is about 7.5 nm, and there are a few

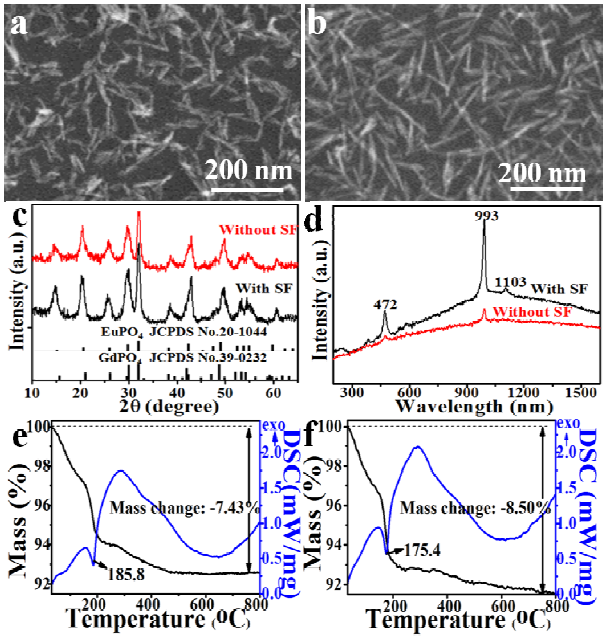

Figure 1. SEM images of $Gd_{0.8}Eu_{0.2}PO_4$ NRs a) without SF and b) with SF, and the inserts are the amplifications of according frame in the images. c) XRD patterns and d) Raman spectra of the as-synthesized $Gd_{0.8}Eu_{0.2}PO_4$ NRs with SF and without SF. TG-DSC curves of the doped NRs e) with SF and f) without SF in the temperature range of 30-800 °C.

irregular fields (marked by the arrows in Figure 2e and 2f), indicating the worse crystallization parts in these NRs. Compared to NRs without SF, the Eu-doped SF-NRs exhibit better dispersion in milliQ water (Figure S4).

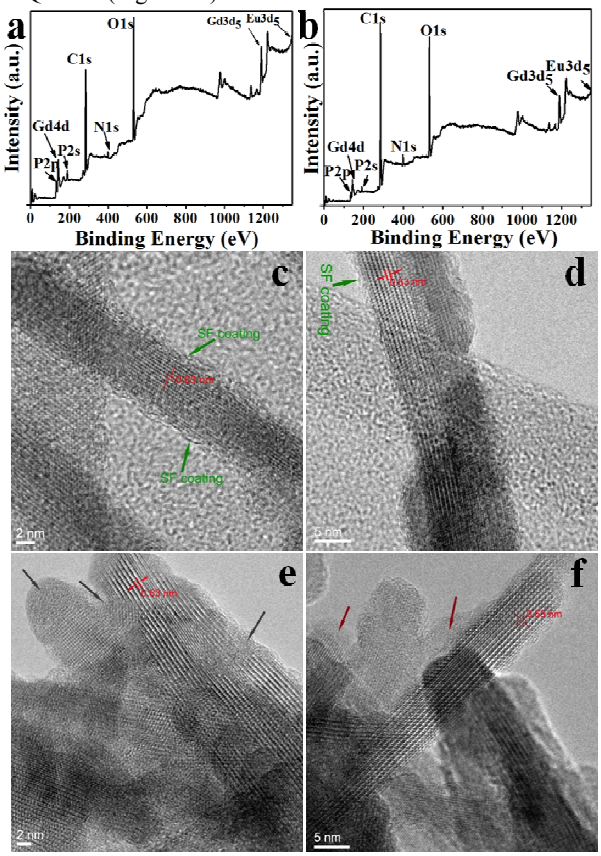

Figure 2. XPS spectra of Eu-doped $GdPO_4$ NRs (a) with SF and (b) without SF, and HRTEM images of the Eu-doped NRs (c, d) with SF and (e, f) without SF.

To insight into the formation mechanism of Eu-doped $GdPO_4$ NRs, the size change of samples in the different preparation time was monitored. The evaluation of the real-time morphology is shown in Figure S5 and S6. Obviously, in the initial stage of reaction (20 min), several NPs and some short nanocrystallites are formed, and their length ranged from 20 to 150 nm (Figure S5a and S6a). After 50 min of reaction, NRs length is increased up to about 50-200 nm (Figure S6b). After 80 min, the length of the NRs is continuously enhanced to about 100-200 nm (Figure S6c). Especially the results in Figure S6 indicate that the length of NRs is obviously increased with the reaction time in the help of SF peptides. Based on these results, the mechanism on the formation of doped $GdPO_4$ NRs via the bio-mineralization process is proposed (Figure 3). In step (a): Gd^{3+} and Eu^{3+} are formed crystal nuclei in the assistance of SF chains, which could provide the more crystallization sites and guided the more crystallization of particles. SF chains with histidine and lysine can be used to synthesize metal-based nanomaterials by a mineralization.[11b] The previous research shows that hydrolyzed SF peptide chains include 4.43% asparagic acid and 1.13% glutamic acid[11c], which can easily be combined with metal ions.[11b-f] On the other hand, 0.17% histidine, 0.79% lysine and 0.90% arginine in hydrolyzed SF peptide chains[11c] can be combined with hydroxyl groups and PO_4^{3-} groups. In step (b): the crystal nuclei in SF chains are slowly mineralized into fine NRs. In Figure S5a, $GdPO_4$ and $EuPO_4$ coated on the primary crystalline nucleus could continuously grow to form fine (shown by the arrows in Figure S5a) and detective hexagonal crystallites with the assistance of SF peptides, in which histidine could form the phosphorus-oxygen bonding and coordination bonding by imidazole groups.[16] In step (c): the SF-linked crystallites continued to grow (Figure S6c) and formed longer hexagonal crystal lanthanide orthophosphate NRs, which are known to exhibit anisotropic growth.[17] In principle, the anisotropic growth of a crystal is favorable for the formation of the thinner NRs[1k,11a]; however, less crystal nuclei are formed in the reaction solution without SF, leading to most shorter NRs obtained in the early growth time (shown in Figure S5); Eu^{3+} ions are reduced into Eu^{2+} ions by tyrosine[15] in SF peptides and Cl^- ions from $EuCl_3$[14], and linked onto the NRs surfaces. On the other hand, the degradation ratios of two kinds of the doped NRs into PBS or FBS (fetal bovine serum) gradually increased from 1 d to 5 d of the immersion time, and the degradation ratios of NRs with/without SF are also different (shown in Figure S7). Especially, the degradation ratios of Eu-doped NRs with SF are lower than those of the doped NRs without SF in the same immersion time, suggesting that SF could prevent NRs from releasing metal ions into PBS, leading to the smaller degradation amounts of SF-NRs in PBS or FBS.

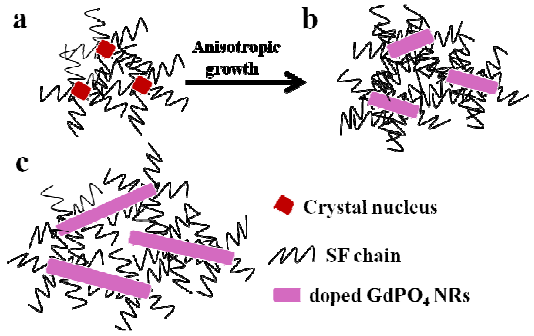

Figure 3. Illustration of Eu-doped $GdPO_4$ growth mechanism in the help of SF peptides: (a) the formation of crystal nuclei in SF chains; (b) nuclei to grow up; (c) larger NRs coalesce to together.

Figure 4a shows the mass magnetic susceptibility value of Eu-doped $GdPO_4$ NRs at 20000 G. The mass magnetic susceptibility value (1.27 emu/g) of Eu-doped NRs with SF is lower than 1.44 emu/g of the NRs without SF, which may result from two factors: first, the interactions of the nitrogen or oxygen atoms in SF chains with the metal ions on the surfaces of NRs induced the surface spin-canting disorder[11a]; secondly, the higher ratio of Eu/Gd in SF-NRs might lead to the lower the magnetization level, compared to NRs without SF. The paramagnetic property of as-prepared NRs comes from seven unpaired inner 4f electrons of Gd^{3+}, which are closely bound to the nucleus and effectively shielded by the outer closed shell electrons $5s^25p^6$ from the crystal field. The magnetic moments associated with Gd^{3+} are all localized and non-interaction, leading to the paramagnetic property of NRs, suggesting that Eu-doped $GdPO_4$ NRs might be applied as MRI contrast agent.[1b] In order to analyze their potential as MRI contrast agents, Eu-doped $GdPO_4$ NRs were assessed for their T_1-weighted images and relaxivity by a 7.0 T MRI system. Figure 4c and 4d show the T_1-weighted imaged in the range of 0-1.0 mM of Gd^{3+} in NRs with/without SF dispersed in agarose solution. With the increase of the Gd^{3+} concentration, the T_1-weighted imaging signal intensities are enhanced, leading to more and more bright images. Furthermore, their relaxivity with the various concentrations were calculated from the slope of the concentration-dependent relaxation rate $1/T_1$ graph. In Figure 4b, the good linear relationship of Gd^{3+} molar concentration again $1/T_1$ exhibits a high effective relaxivity r_1 value of 1.38 (Gd mM·s)$^{-1}$ of SF-NRs; however, the r_1 value of the doped NRs without SF is only 0.912 (Gd mM·s)$^{-1}$. The higher r_1 value of SF-NRs result from several factors: Gd^{3+} ions on the surfaces of SF-NRs could also be

linked with nitrogen and carboxyl oxygen in the SF chains, leading to the necessary water molecule coordinating to Gd^{3+} ions[18] and the larger rotational correlation time, giving the larger relaxivity[19]; the doping of the more Eu ions with smaller magnetic moments, which could partly be linked with the OH and NH groups in SF chains, leading to the large shift in the resonance of the nuclei surrounding the Eu ions and the more efficient transfer of the magnetization,[19], especially the appearance of the more Eu^{2+} (Figure S3a) indicate that SF-NRs might be used as a stable redox active Eu-based MRI contrast agent[4b,7]; the thinner diameter of SF-NRs could give rise to the larger specific surface area, leading to their higher mole relaxivity,[4b,20] because Gd^{3+} ions at and near the outer surface should contribute more to the relaxivity than ions in the inside of particles.[4b,21] Then, their T_1 weighted MR imaging capability *in vivo* was further evaluated. As shown in Figure 4e, a significant brightening in the T_1–weighted MR image was observed at the tumor site after Eu-doped SF-NRs were injected, and through the T_1 signal intensity measurement of a serial of MR images of pre- and post-injections, it is obtained that the average brightness of post-injection in tumor site is increased about 53.00 %. These results indicate that the Eu-doped $GdPO_4$ SF-NRs have better potential as the T_1 contrast agent for MRI, compared with the Eu-doped NRs without SF.

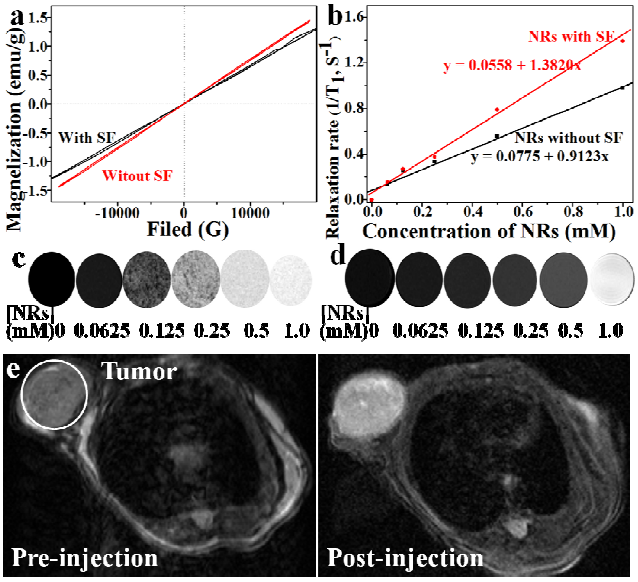

Figure 4. (a) Hysteresis of prepared Eu-doped $GdPO_4$ NRs, (b) plot of relaxation rate ($1/T_1$) and T_1-weighted MR images of Eu-doped $GdPO_4$ NRs (c) with SF and (d) without SF at various Gd^{3+} concentrations in 0.5% agarose aqueous solution. e) *In vivo* T_1-weighted MR images of a tumor-bearing mice before and after injecting Eu-doped $GdPO_4$ SF-NRs.

The images of L929 cells treated with SF-NRs or NRs without SF under different concentrations for 1d (seen in Figure S8) reveal that, many cells contacted with SF-NRs, many cells at the lower NR concentrations (25 and 50 μg/mL) could keep their good morphology. MTT assays in Figure 5a–c show the L929 surviving fraction in the different NR suspensions. When the cells were cultured with NRs for 1 d, SF-NRs could promote significantly the viability of cells at the concentration of 25, 50, 100 and 200 μg/mL (in Figure 5a); however, NRs without SF could not promote the viability of cells in the concentration of 50, 100, 200 μg/mL, because NRs might provide more metal ions into cell viability at higher concentration of NRs. Similarly, when the cells are cultured with NRs for 3 d, SF-NRs obviously promote the viability at their various concentrations; however, NRs without SF significantly inhibited the viability of cells at the concentration of 100 and 200 μg/mL (Figure 5b). When the cells were cultured with NRs for 5 d, SF-NRs obviously promoted the viability at the concentration of 25 and 200 μg/mL; however, NRs without SF significantly inhibited the viability of cells at their various concentrations (Figure 5c), because SF peptide coating could slow the release of metal ions from SF-NRs in PBS and FBS (fetal bovine serum, Figure S7). Compared to NRs without SF, SF-NRs could significantly promote the viability of cells at the concentration from 25 to 200 μg/mL (Figure 5a and b). The length distributions of SF-NRs before and after cell internalization were analyzed (Figure 5d). Each distribution was determined from more than 100 NRs. It can be found that the cell-internalized NRs are slightly shorter than their initial form, suggesting that the internalization of NRs is optimized when their length corresponds to the average size of the adherent cells.[14a] The ultrathin section of L929 cells cultured with 100 μg/mL of NRs for 3d were observed using TEM (Figure S9). It is clear that the prepared NRs (marked by red arrows) are internalized inside of L929 cells. In Figure S9a and c, although nuclei and mitochondria are observed, their karyotheca is vague, and many vacuoles appeared in Figure S9a, indicating that NRs without SF negatively influence the cells activity. However, in Figure S9b and d, the cell membranes and karyotheca remain integral, and an integral mitochondria is clearly observed, indicating that the cell is very vivid. These results indicate that SF peptides on Eu-doped $GdPO_4$ could promote NRs to enter into cells and improve the cyto-compatibility of the prepared NRs, which is consistent with the result of MTT.

Although Eu^{3+} ions in the body are toxic,[22] low toxic SF-NRs are fabricated in our study, and they do not have significantly negative influence on cell viability under their different concentrations and culture time of L929 cells. Obviously, SF peptide coating could reduce the toxicity of NRs upon L929 cells, which may be explained by the following reasons. First, SF peptides could help NRs to enter into cells, avoiding the damage of the cells membrane and karyotheca.[23] Second, the chelation of metal ions on the NR surface with histidine or lysine in SF chains could reduce the production of radical oxygen species,[24] consequently decreasing the membrane lipid peroxidation at the cellular level and organelle level, especially keeping high activity of mitochondria[11d,c], and avoiding the apoptosis of L929 cells. Third, SF peptides could slow the release of metal ions (Figure S7), avoiding the higher concentration

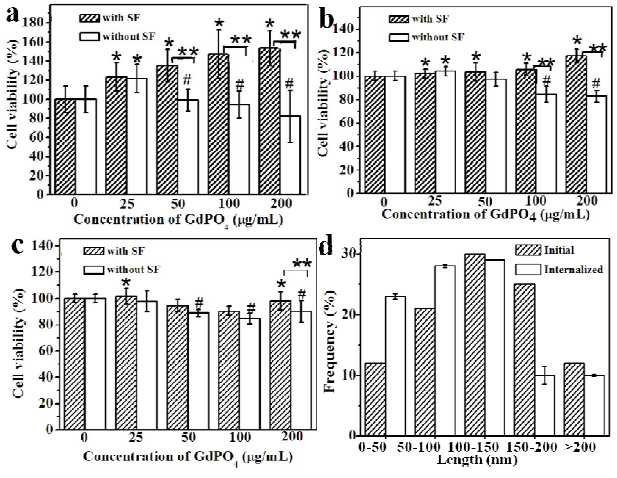

Figure 5. Cell viability of L929 cells incubated with Eu-doped $GdPO_4$ NRs of different concentrations for (a) 1 d, (b) 3 d and (c) 5 d (* shows significant difference with control group, # shows obvious inhibition with control group, **shows significant difference between two corresponding groups, $p < 0.05$, n=3); (d) Length distributions of initial SF-NRs and their internalized forms.

accumulation of excessive metal ions inside cell and apoptosis of cells.[11f] Besides, SF can also decrease the direct contact area between cellular organelle and the crystallites of SF-NRs. As a result, SF-NRs could reduce the asbestos toxicity.

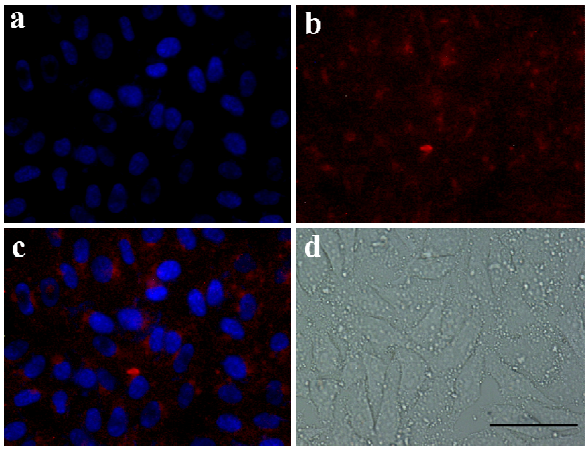

Figure 6. The dark and overlapped background images under violet excitation (a-c) and the bright image (d) of HepG2 cells with Eu-doped $GdPO_4$ NRs, and the bar is 50 μm.

As presented in Figure S10 and S11, Eu-doped $GdPO_4$ with SF showed good photoluminescence properties. Furthermore, the optical probe application of Eu-doped $GdPO_4$ NRs in the luminescence imaging of living cells was carried out through the inverted fluorescence microscope under violet (wavelength of ~410 nm) excitation. After cells were incubated with 150 μg/mL SF-NRs for 8 h at 37 ^oC, these SF-NRs clearly retained their intrinsic luminescent properties in cellular internalization. The blue nuclei stained by Hochest in Figure 6a present cell number, and many pink fields from the violet excitation in Figure 6b indicate the distribution and aggregation of Eu-doped NRs outside/inside the cells. The overlay of the luminescence images in Figure 6c shows that the strong pink luminescence was clearly observed from cells. Bright field image in Figure 6d shows that many SF-NRs have contacted with or entered into cells with the integrated morphology, even the pink SF-NRs inside cells have contacted with the nuclei. However, in Figure S12, there are weaker pink fields (from the same violet excitation and the same conditions of cell test) in the overlay of the luminescence images of the co-culture between cells and the Eu-doped NRs without SF. This result should be due to the fact that SF coating improves SF-NRs to enter into cells and to contact with the proteins inside the cells, enhancing the Eu ions emission in presence of the proteins.[8] These results suggest that the as-prepared SF-NRs are promising candidates for use in cell imaging.

Conclusions

In this work, a fast and simple mineralization technique is developed for the synthesis of Eu-doped $GdPO_4$ SF-NRs under the assistance of SF peptides. The analysis results showed that these as-prepared NRs had hexagonal crystalline structure, and the length and diameter of the Eu-doped $GdPO_4$ SF-NRs are ~150 nm and ~10 nm, respectively. The results of Raman, FTIR, TG-DSC and XPS proved that the as-prepared NRs are conjugated with SF chains and doped with Eu ions. The Eu-doped $GdPO_4$ SF-NRs have strong pink luminescence and 1.27 emu/g of the mass magnetic susceptibility value at 20000 G of magnetic field. SF-NRs obviously promote the viability of cells at NRs concentration of 25-200 μg/mL for 1 and 3 d cells, and SF-NRs have better cyto-compatibility due to SF peptide coating on NRs and lesser release of metal ions from SF-NRs. A primary growth mechanism of Eu-doped $GdPO_4$ NRs in the template of SF is proposed, in which SF coating not only promotes the cyto-compatibility of SF-NRs, but also leads to the higher luminescence inside the cells, high longitudinal relaxivity r_1 value of 1.38 (Gd $mM \cdot s)^{-1}$ and *in vivo* T_1 weighted MR imaging enhancement. Based on their properties, Eu-doped $GdPO_4$ SF-NRs would have the potential applications in the biomedical field, such as T_1 MRI and optical imaging.

Experimental Section

The silk was boiled for 30 min in a 0.3% Na_2CO_3 solution to degum, then hydrolyzed in 6 M HCl (10 mL) at 80 ^oC for 24 h. The hydrolyzed solution was adjusted to pH 7 and dialyzed with distilled water for 24 h at room temperature. Finally, the dialyzed SF solution was collected and its concentration was adjusted to 0.02 mg/mL with distilled water.

The $GdPO_4$ NRs were prepared via a mild mineralization process with the help of SF. In a typical synthesis of $GdPO_4$ NRs, aqueous solution of $Gd(NO)_3$ (20 mL, 0.5 M) and SF solution (1.05 mL, 0.02 mg/mL) were added into a 250 mL beaker. Then a solution of NaH_2PO_4 (10 mL, 1 M) was slowly added drop by drop into above solution under vigorous stirring for 20 min, until the mixture solution was milky, then was kept at 80 ^oC for 5 h. The white precipitate was washed three times with distilled water and absolute alcohol, respectively, in order to remove surplus metal ions, and finally dried at 60 ^oC in air overnight for their further utilization. A control sample was prepared in the SF-free solution in order to analyze the effect of SF peptide in the preparation process. In order to obtain Eu-doped $GdPO_4$ NRs, 10, 20, 30 mol% of $Gd(NO_3)_3$ were substituted by $EuCl_3$ during the above mineralization process.

Acknowledgments

This work has been supported by the National Natural Science Foundation of China (project No. 51273122, 51173120, 51372157 and 51202151). The supports of Key Project of National Natural Science Funding (81130027) and The National Basic Research Program of China (973 Program, 2011CB935804) are also acknowledged with gratitude.

Notes and references

[a] College of Materials Science and Engineering, Sichuan University, Chengdu, 610065, People's Republic of China.
Email: zbhuang@scu.edu.cn; Fax: 86-28-85413003; Tel: 86-28-85413003
[b] Laboratory of Controllable Preparation and Application of Nanomaterials, Research Center for Micro&Nano Materials and Technology, Technical Institute of Physics and Chemistry, Chinese Academy of Sciences, Beijing 100190, People's Republic of China.
E-mail: mengxw@mail.ipc.ac.cn; Fax: +86-10-62554670; Tel: +86-10-82543521
[c] Molecular Imaging Center, Department of Radiology, West China Hospital of Sichuan University, Address: No.2, 4th Keyuan Road, Chengdu, 610093, China.

† Footnotes should appear here. These might include comments relevant to but not central to the matter under discussion, limited experimental and spectral data, and crystallographic data.

Electronic Supplementary Information (ESI) available: [details of any supplementary information available should be included here]. See DOI: 10.1039/c000000x/

† Footnotes should appear here. These might include comments relevant to but not central to the matter under discussion, limited experimental and spectral data, and crystallographic data.
Electronic Supplementary Information (ESI) available: [details of any supplementary information available should be included here]. See DOI: 10.1039/c000000x/

1 a) A. I. Becerro, S. Rodríguez-Liviano, A. J. Fernández-Carrión and M. Ocaña, *Cryst. Growth Des.,* 2013**, 13***,* 526; b) W. Ren, G. Tian, L. Zhou, W. Yin, L. Yan, S. Jin, Y. Zu, S. Li, Z. Gu and Y. Zhao, *Nanoscale,* 2012**, 4**, 3754; c) B. Abécassis, F. Lerouge, F. Bouquet, S. Kachbi, M. Monteil and P. Davidson, *J. Phys. Chem. B,* 2012**, 116***,* 7590; d) M. Yang, H. You, Y. Liang, J. Xu, F. Lu, L. Dai and Y. Liu, *J. Alloy. Compd.,* 2014, **582**, 603; e) N. Yaiphaba, R. S. N. ShantaSingh, R. K. Vatsa and N. RajmuhonSingh, *J. Lumin.,* 2010, **130**, 174; f) L. Yu, D. Li, M. Yue, J. Yao and S. Lu, *Chem. Phys.,* 2006, **326,** 478; g) H. Assaaoudia, A. Ennaciria and A. Rulmont, *Vib. Spectrosc.,* 2001, **25,** 81; h) M. Guan, F. Tao, J. Sun and Z. Xu, *Langmuir,* 2008, **24**, 8280; i) L. D. Mengistie, A. Duarte, L. C. P. Sonia, F. G. C. G. Carlos, D. C. Luis and R. Joao, *Nanoscale,* 2012**, 4**, 5154; j) K. Park, M. H. Heo, K.Y. Kim, S. J. Dhoble, Y. Kim and J. Y. Kim, *Powder Technol.,* 2013**, 237**, 102; k) C. R. Patra, G. Alexandra, S. Patra, D. S. Jacob, A. Gedanken, A. Landau and Y. Gofer, *New J. Chem.,* 2005, **29,** 733; l) A. Louie, *Chem. Rev.,* 2010, **110,** 3146.

2 a) K. Riwotzki, H. Meyssamy, A. Komowski and M. Haase, *J. Phys. Chem. B,* 2000, **104,** 2824; b) G. Carini, G. D´. Angelo, G. Tripodo, A. Fontana, F. Rossi and G. A. Saunders, *Europhys. Lett.,* 1997, **40**, 435; b) H. Meyssamy and K. Riwotzki, *Adv. Mater.,* 1999, **11**, 840; c) A. W. Xu, Y. P. Fang, L. P. You and H. Q. Lin, *J. Am. Chem. Soc.,* 2003, **125**, 1494.

3 a) J. Cheon and J. H. Acc. Lee, *Chem. Res.,* 2008, **41**, 1630; b) M. N. Luwang, R. S. Ningthoujam, Jagannath, S. K. Srivastava and R. K. Vatsa, *J. Am. Chem. Soc.,* 2010, **132**, 2759; c) M. N. Luwang, R. S. Ningthoujam, S. K. Srivastava and R. K. Vatsa, *J. Am. Chem. Soc.* 2011, **133**, 2998; d) R. S. Ningthoujam, *Pramana – J. Phys.,* 2013, **80**, 1055.

4 a) M. Bottrill, L. Kwok and N. J. Long, *Chem. Soc. Rev.,* 2006, **35**, 557; b) Y. Li, T. Chen, W. Tan and D. R. Talham, *Langmuir*, 2014, **30**, 5873.

5 K. Riwotzki, H. Meyssamy, H. Schnablegger, A. Komowski and M. Haase, *Angew. Chem. Int. Ed.,* 2001, **40**, 573.

6 a) H. Hifumi, S. Yamaoka, A. Tanimoto, D. Citterio and K. Suzuki, *J. Am. Chem. Soc.,* 2006, **128,** 15090; b) H. Hifumi, S. Yamaoka, A. Tanimoto, T. Akatsu, Y. Shindo, A. Honda, D. Citterio, K. Oka, S. Kuribayashi and K. Suzuki, *J. Mater. Chem.,* 2009, **19,** 6393.

7 a) L. Burai, E. Tóth, S. Seibig, R. Scopelliti and A. E. Merbach, *Chem.-Eur. J.*, 2000, **6,** 3761; b) R. S. Ningthoujam, V. Sudarsan, R. K. Vatsa, R. M. Kadam, Jagannath and A. Gupta, *J. Alloy. Comp.,* 2009, **486**, 864.

8 J. Hamblin, N. Abboyi and M. P. Lowe, *Chem. Commun.*, 2005, 657.

9 a) A. J. Villaraza, A. Bumb and M. W. Brechbiel*, Chem. Rev.***,** 2010*,* **110,** 2921; b) E. Scoffone, A. Fontana and R. Rocchi, *Biochemistry,* 1968**, 7**, 971.

10 a) Y. Xia, P. Yang, Y. Sun, Y. Wu, B. Mayers, B. Gates, Y. Yin, F. Kim and H. Yan, *Adv. Mater.,* 2003, **15**, 353; b) N. KrÖger, M. B. Dickerson, G. Ahmad, Y. Cai, M. S. Haluska, K. H. Sandhage, N. Poulsen and V. C. Sheppard, *Angew. Chem. Int. Ed.,* 2006, **45**, 7239; c) S. -Y. Lee, X. Gao and H. Matsui, *J. Am. Chem. Soc.* 2007, **129**, 2954.

11 a) Z. Huang, D. Yan, M. Yang, X. Liao, Y. Kang, G. Yin, Y. Yao and B. Hao, *J. Colloid Interf. Sci.,* 2008, **325,** 356; b) D. Yan, G. Yin, Z. Huang, M. Yang, X. Liao, Y. Kang, Y. Yao, B. Hao and D. Han, *J. Phys. Chem. B,* 2009, **113,** 6047; c)D. Yan, G. Yin, Z. Huang, X. Liao, Y. Kang, Y. Yao, B. Hao, J. Gu and D. Han, *Inorg. Chem.,* 2009, **48**, 6471; d) Y. Wang, X. Liao, Z. Huang, G. Yin, J. Gu and Y. Yao, *Colloid. Surf. A.,* 2010, **372,** 165; e) D. Yan, G. Yin, Z. Huang, L. Li, X. Liao, X. Chen, Y. Yao and B. Hao, *Langmuir,* 2011, **27,** 13206; f) J. Liu, M. Deng, Z. Huang, G. Yin, X. Liao and J. Gu, *Colloid. Surf. B.,* 2013, **107,** 19.

12 M. F. Dumont, C. Baligand, Y. Li, E.S. Knowles, M.W. Meisel, G. A. Walter and D. R. Talham, *Bioconjugate Chem*., 2012, **23,** 951.

13 N. K. Sahu, R. S. Ningthoujam and D. Bahadur, *J. Appl. Phys.,* 2012, **112,** 014306.

14 a) A. Kelly, G. W. Groves and P. Kidd, Crystallography and Crystal Defects, Revised ed., Wiley, New York, 2000; b) F. Le, L. Wang, W. Jia, D. Jia and S. Bao, *J. Alloy. Comp.* 2012, **512**, 323.

15 a) J.G. Metz, P. J. Nixon, M. Rögner, G. W. Brudvig and B. A. Diner, *Biochemistry* 1989, **28**, 6960; b) B.A. Diner, D. A. Force, D. W. Randall and R. D. Britt, *Biochemistry* 1998, **37,** 17931.

16 a) J. Zhao, Z. Huang, J. Zeng, M. Deng, G. Yin, X. Liao and J. Gu, *J. Inorg. Organomet. Polym.* 2012, **22**, 492; b) G. Yin, Z. Huang, M. Deng, J. Zeng, J. Gu, *J. Colloid Interf. Sci.* 2011, **363**, 393; c) M. Safi, M. Yan, M.-A. Guedeau-Boudeville, H. Conjeaud, V.; Boggetto, N. Garnier-Thibaud, A. Baeza-Squiban, F. Niedergang, D. Averbeck and J.-F. Berret, *ACS Nano,* 2011, **7**, 5354.

17 Z. A. Peng and X. G. Peng, *J. Am. Chem. Soc.,* 2002, **124**, 3343.

18 J. J. Stezokowski and J. L. Hoard, *Isr. J. Chem.*, **1984**, *24*, 323.

19 S. Aime, C. Carrera, D. D. Castelli, S. G. Crich and E. Terreno, *Angew. Chem., Int. Ed.*, 2005, **44**, 1813.

20 A. T. M. A. Rahman, P. Majewski and K. Vasile, *Media Mol. Imag.,* 2013, **8,** 92.

21 a) V. Kubicek, J. Rudovsky, J. Kotek, P. Hermann, L. V. Elst, R. N. Muller, Z. I. Kolar, H. T. Wolterbeek, J. A. Peters and I. Lukes, *J. Am. Chem. Soc.*, 2005, **127,** 16477; b) W. J. Rieter, K. M. L. Taylor, H. An, W. Lin and W. Lin, *J. Am. Chem. Soc*., 2006, **128,** 9024.

22 K. Binnemans, *Chem. Rev.*, 2009, **109,** 4283.

23 a) A. Picot, A. D'Aléo, P. L. Baldeck, A. Grichine, A. Duperray, C. Andraud and O. Maury, *J. Am. Chem. Soc.*, 2008, **130,** 1532; (b) L. Burai, E. Tóth, G. Moreau, A. Sour, R. Scopelliti and A. E. Merbach, *Chem.-Eur. J.*, 2003, **9**, 1394.

24 a) A. Chiarini, P. Petrini, S. Bozzini, P. Dal and U. Armato, *Biomaterials,* 2003**, 24,** 789; b) N. Minoura, S. Aiba, M. Higuchi, Y. Gotoh, M. Tsukada and Y. Imai, *Biochem. Biophys. Res. Commun.,* 1995, **208,** 511.

The hexagonal crystal Eu−doped $GdPO_4$ NRs coated by silk fibroin have been prepared in the template of silk fibroin (SF) peptides via a mineralization process. A growth mechanism of Eu-doped $GdPO_4$ SF-NRs is proposed, to explain their stronger pink luminescence and better cyto-compatibility. Eu-doped SF-NRs exhibit a higher longitudinal relaxivity r_1 value of 1.38 (Gd mM·s)$^{-1}$ and the better luminescence imaging of living cells.